



Contents lists available at ScienceDirect

Science of the Total Environment

journal homepage: www.elsevier.com/locate/scitotenv

Inorganic markers, carbonaceous components and stable carbon isotope from biomass burning aerosols in Northeast China

Fang Cao^{a,b,1}, Shi-Chun Zhang^{c,1}, Kimitaka Kawamura^b, Yan-Lin Zhang^{a,b,*}

^a Yale-NUIST Center on Atmospheric Environment, Nanjing University of Information Science and Technology, Nanjing 10044, China

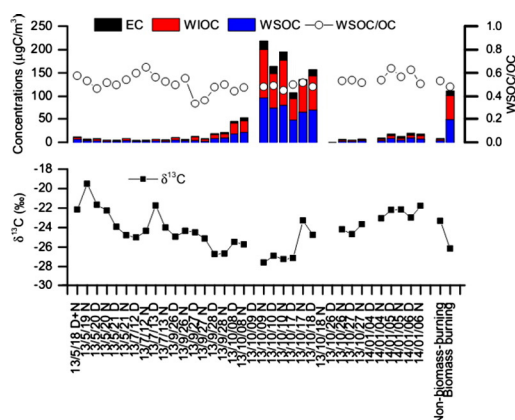
^b Institute of Low Temperature Science, Hokkaido University, N19 W08, Kita-ku, Sapporo 060-0819, Japan

^c Northeast Institute of Geography and Agroecology, Chinese Academy of Sciences, 4888 Shengbei Road, Changchun 130102, China

HIGHLIGHTS

- Open biomass burning episodes are identified in Sanjiang Plain, NE China.
- K^+ and $PM_{2.5}$ are increased significantly during the biomass burning periods.
- The biomass burning aerosols are mostly fresh emitted and less-aged.
- A lower average $\delta^{13}C$ value (-26.2%) is found for the biomass-burning aerosols.
- Biomass-burning aerosols in Sanjiang are mainly from the combustion of C3 plants.

GRAPHICAL ABSTRACT



ARTICLE INFO

Article history:

Received 20 June 2015

Received in revised form 8 September 2015

Accepted 18 September 2015

Available online xxxx

Editor: J. P. Bennett

Keywords:

Aerosol

Biomass burning

Stable carbon isotope

Source

Potassium

ABSTRACT

To better characterize the chemical compositions and sources of fine particulate matter (i.e. $PM_{2.5}$) in Sanjiang Plain, Northeast China, total carbon (TC), organic carbon (OC), elemental carbon (EC), water-soluble organic carbon (WSOC), and inorganic ions as well as stable carbon isotopic composition ($\delta^{13}C$) were measured in this study. Intensively open biomass burning episodes are identified from late September to early October by satellite fire and aerosol optical depth maps. During the biomass-burning episode, concentrations of $PM_{2.5}$, OC, EC, and WSOC are increased by a factor of 4–12 compared to those during the non-biomass-burning period. Non-sea-salt potassium is strongly correlated with $PM_{2.5}$, OC, EC and WSOC, demonstrating an important contribution from biomass-burning emissions. The enrichment in both the non-sea-salt potassium and chlorine is significantly larger than other inorganic species, suggesting that biomass-burning aerosols in Sanjiang Plain are mostly fresh and less aged. In addition, the WSOC-to-OC ratio is lower than that reported in biomass-burning aerosols in tropical regions, further supporting that biomass-burning aerosols in Sanjiang Plain are mostly primary and secondary organic aerosols may be not significant. A lower average $\delta^{13}C$ value (-26.2%) is observed during the biomass-burning period, indicating a dominant contribution from combustion of C3 plants in the studied region.

© 2015 Published by Elsevier B.V.

* Corresponding author at: Yale-NUIST Center on Atmospheric Environment, Nanjing University of Information Science and Technology, Nanjing 10044, China.

E-mail address: dryanlinzhang@gmail.com (Y.-L. Zhang).

¹ These authors contribute equally to this work.

1. Introduction

Carbonaceous aerosols such as organic carbon (OC) and elemental carbon (EC) contribute from 10% up to 90% of the total mass of fine aerosols (particulate matter with a diameter $<2.5 \mu\text{m}$ or $\text{PM}_{2.5}$), affecting local/regional air quality, human health, the Earth's climate (Pöschl, 2005; Pope III and Dockery, 2006; Jimenez et al., 2009; IPCC, 2013). Biomass burning such as wildfires, agricultural waste burning and bio-fuel combustion can contribute to large amounts of OC and EC in the atmosphere (Andreae and Merlet, 2001; Zhang et al., 2010a; Sang et al., 2013; Rajput et al., 2014; Zhang et al., 2014). In China, the annual amount of burnt straws is $\sim 140 \text{ Tg}$, accounting for 23.3% of total crop production, with larger burned areas in the provinces in eastern and northeast regions (Cao et al., 2008). The importance of biomass burning aerosols has already been underlined by many literatures, most of which have been conducted in Southeast and North China such as the North China Plain, the Yangtze River Delta, and the Pearl River Delta regions (Zhang et al., 2010b; Cheng et al., 2013; Huang et al., 2013; Kawamura et al., 2013; Cheng et al., 2014; Qin et al., 2014). However, little is known about the chemical compositions of biomass burning aerosols in Northeast China despite the large burned crop waste in this region.

The Sanjiang Plain is one of the most productive agricultural regions in China (Wang et al., 2011). During the harvest seasons, burning of agricultural residues is a very common practice in this region, which has been evident by the Moderate Resolution Imaging Spectroradiometer (MODIS) fire count data (Qin et al., 2014). However, few studies have reported the chemical and isotopic compositions of biomass burning aerosols in this region. Source characterization of carbonaceous aerosols over Northeast China especially during biomass burning period is still not well understood, and the contribution of biomass burning is therefore very uncertain.

Stable carbon ($\delta^{13}\text{C}$) isotopic compositions can provide important information about sources and atmospheric processes of carbonaceous aerosol (Martinelli et al., 2002; Widory et al., 2004; Fisseha et al., 2009; Fu et al., 2012). The $\delta^{13}\text{C}$ in total carbon (TC) derived from C4 plants (mean: -13.5‰) is much higher than that emitted from C3 plants (mean: -30.5‰) (Martinelli et al., 2002) and this difference is due to different kinetic isotope effects occurring in the carbon fixation processes for C3 and C4 plants (Tiunov, 2007). Based on stable carbon isotopic compositions, a recent study has revealed that burning C3 plants on average contribute to 59% of TC of $\text{PM}_{2.5}$ in Tanzania (Mkoma et al., 2014). However, stable carbon isotope analysis of aerosol has been less reported in China especially in rural and background sites. To our knowledge, previous studies have been only carried out at urban sites (Cao et al., 2013; Dai et al., 2015). For example, using stable carbon isotope data in both the organic carbon (OC) and elemental carbon (EC), Cao et al. (2013) revealed that fossil fuel combustions were dominant sources for carbonaceous $\text{PM}_{2.5}$ in Shanghai. Stable carbon isotope ratio measurements in combination with measurements of biomass burning markers (e.g. water-soluble potassium) is expected to provide new insights into characteristics and composition of atmospheric aerosols from different sources (Kundu et al., 2010; Mkoma et al., 2014).

In this paper, we present the measurement results on inorganic markers, carbonaceous components and the stable carbon isotope composition in $\text{PM}_{2.5}$ collected at a rural background site in Sanjiang Plain, Northeast China from May 2013 and Jan. 2014. Specifically, mass concentrations of major components in $\text{PM}_{2.5}$ such as inorganic ions, OC, EC and water-soluble OC (WSOC) as well as stable carbon isotope composition of TC during biomass-burning and non-biomass-burning events are compared. Contribution from combustion of C3 and C4 plant during biomass-burning period is also quantified. The results obtained from this study could be beneficial for a more accurate understanding of biomass burning aerosols in China.

2. Experimental

2.1. Study site

The study was conducted in the Sanjiang Plain in northeast China, which is an alluvial plain formed by three major rivers including the Songhua River, the Heilong River, and the Wusuli River. The Sanjiang Plain was historically the largest freshwater wetland in China with densely distributed marsh vegetation coverage. However, this area was reclaimed for many times due to intensive cultivation during the last 50 years (Wang et al., 2011). The rice paddy area was increased 161.5% from 1986 to 2005 and become one of most important agriculture regions of China (Wang et al., 2011; Zhao et al., 2015). Agricultural residues burring after harvesting is a common practice in this region and may produce large amounts of air pollutants. The experimental site is located at the Sanjiang Marsh Wetland Ecological Experimental Station, Chinese Academy of Sciences ($47^{\circ}35\text{N}$, $133^{\circ}31\text{E}$), 80 km away southeast Tongjiang City, Heilongjiang Province ($47^{\circ}67\text{N}$, $132^{\circ}50\text{E}$) (Fig. 1). The annual mean temperature is 1.5 to 4.0°C with the highest and lowest temperatures in July and January, respectively. The haze episodes or smog days accompanied by the reduced visibility and high aerosol mass concentration have been often observed, which may be associated with agricultural waste openly burning in autumn especially from the end of September to the beginning of October. In this study, $\text{PM}_{2.5}$ aerosol samples were collected on prebaked quartz filters ($25 \times 20 \text{ cm}$) for a day/night basis (07:00–18:00 LT for daytime and 18:00–06:00 LT for nighttime) by a high volume air sampler (Tianhong Co., Wuhan, China) at a flow rate of $1.05 \text{ m}^3/\text{min}$. In total, 36 $\text{PM}_{2.5}$ samples were collected, in which 10 samples were collected during intensive open field burning days. After sampling, the filters were wrapped in aluminum foils, packed in air-tight polyethylene bags and stored at -20°C for analysis. 4 field blank filters were also collected, following 10 min exposures to ambient air without active sampling. $\text{PM}_{2.5}$ mass concentration was analyzed gravimetrically (Sartorius MC5 electronic microbalance) with $\pm 1 \mu\text{g}$ sensitivity before and after sampling (at 25°C and $45 \pm 5\%$ during the weighing).

2.2. Chemical analysis

To determine the inorganic ions, a 1.4 cm diameter disk of a filter sample was extracted with 10 ml ultrapure water in a plastic vial using an ultrasonic bath for 15 min for 2 times. The water extracts were filtered using a disk filter (Millex-GV, $0.22 \mu\text{m}$, Millipore). The major ions including SO_4^{2-} , NO_3^- , Cl^- , MSA^- , NH_4^+ , K^+ , Ca^{2+} , Mg^{2+} , and Na^+ were measured using an ion chromatograph (761 Compact IC, Metrohm, Switzerland). The analytical errors from duplicate analysis were within 5%. The field blanks for Na^+ and Ca^{2+} as well as MSA^- , Cl^- , NO_3^- and SO_4^{2-} are 0.090, 0.120, 0.004, 0.010, 0.001 and 0.010 ng/L , respectively.

For the determination of water-soluble organic carbon (WSOC), a 2.0 cm disk of the filter sample was extracted with 12 ml organic-free ultrapure water in a glass vial using an ultrasonic bath for 30 min. The water extracts were passed through a disk filter (Millex-GV, $0.22 \mu\text{m}$, Millipore) and WSOC was then measured using a TOC analyzer (Shimadzu, TOC-V_{CSH}, Japan). The analytical errors from triplicate analysis of laboratory standards were smaller than 5%.

The mass concentrations of OC and EC were measured using a thermal/optical OC/EC analyzer (Sunset Laboratory, USA) with NIOSH protocol (Birch and Cary, 1996), which has been described in details elsewhere (Jung and Kawamura, 2011). The analytical errors (i.e., the precision of the measurement) from duplicate analysis of the filter samples were less than 6% for OC and 5% for EC.

TC in aerosol samples and their stable carbon isotopic ratio were determined using an elemental analyzer (EA) (Carlo Erba, NA 1500) coupled with an isotope ratio mass spectrometer (IRMS, Finnigan MAT

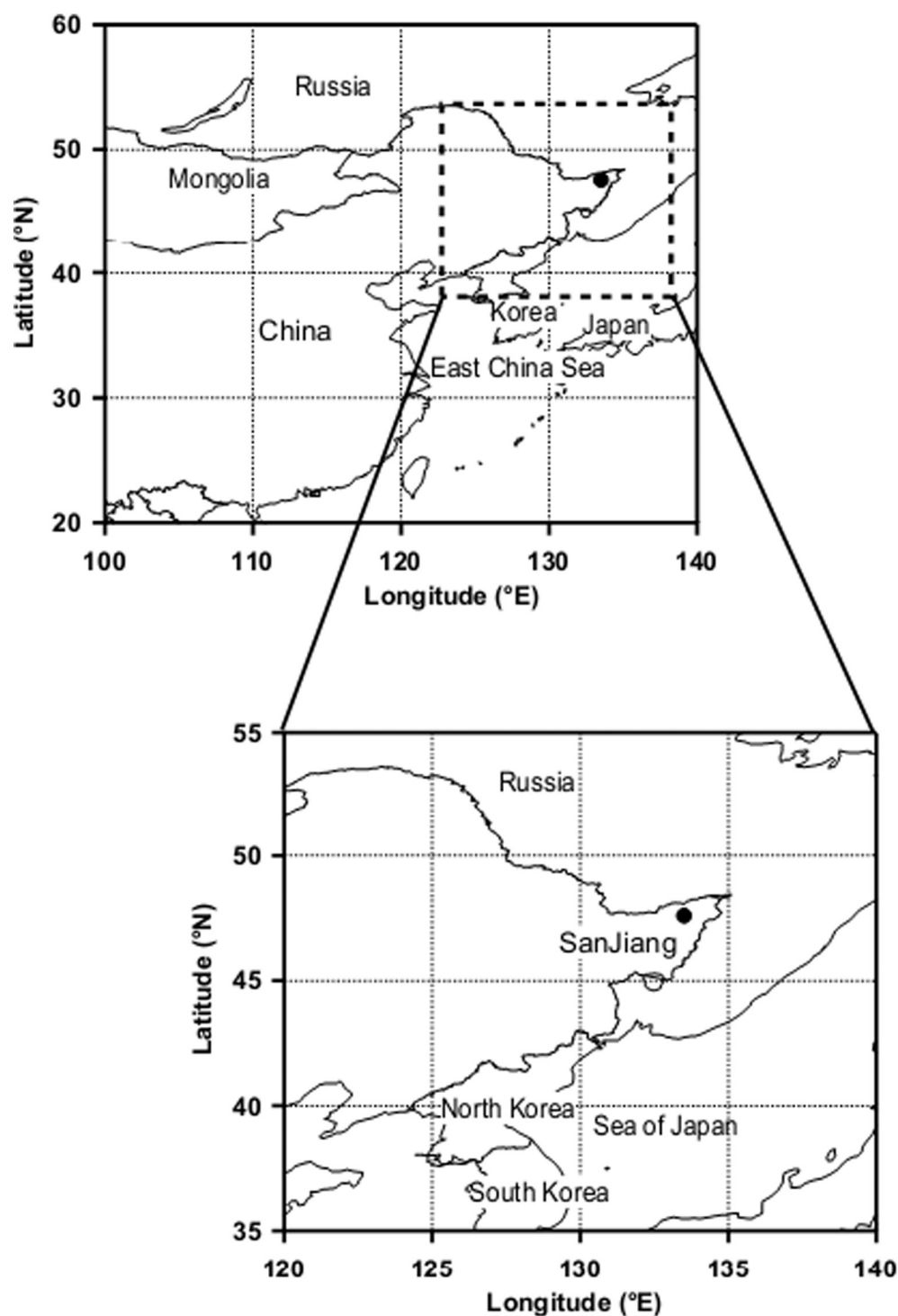


Fig. 1. A sampling location in the Sanjiang Plain, Northeast China.

Delta Plus) (Jung and Kawamura, 2011). A filter disk of 1.6 cm diameter was packed in a tin cup, loaded into the EA by an auto-sampler and then oxidized by chromium (III) oxide at 1020 °C. The resulting CO₂ was purified by an online GC column equipped in the EA and then measured with a thermal conductivity detector. A small aliquot of CO₂ gas was introduced to the IRMS through an interface ConFlo II (ThermoQuest). The carbon isotopic composition is expressed as $\delta^{13}\text{C}$, which is relative to the Pee Dee Belemnite (PDB). External calibration was conducted using five known amounts (ranging from 0.2 to 0.6 mg) of acetanilide (Thermo Scientific) with known $\delta^{13}\text{C}$ of TC (−27.26‰). The analytical errors of $\delta^{13}\text{C}$ based on the duplicate analyses were less than 0.1%. TC

concentrations measured with EA agree well ($p < 0.01$) with that measured with an OC/EC analyzer.

3. Results and discussion

3.1. General description of biomass burning episodes

As illustrated in Fig. 1, remarkably high concentrations of PM_{2.5} and Water-soluble potassium (K⁺) were identified during the early October, which was a typical biomass burning season in this region. To validate the occurrence of extensive open biomass burning, a fire map detected

by MODIS on the NASA's Terra and Aqua satellites (the integrated data are available at the website of the University of Maryland: <http://maps.geog.umd.edu/products.asp>) over the Northeast China was shown in Fig. 3. During the pollution episode, the fire counts map indicates the biomass burning activities in Northeast Asia (mainly in the Heilong Jiang province) was very extensive. Moreover, MODIS observations on Oct. 9/10 (when peak $PM_{2.5}$ mass concentration is observed) show a large area of aerosols optical depth (AOD) at 550 nm >0.6 over the fires (Fig. 3).

It should be noted that open crop residue burning in autumn (starting from late September and lasting for 2–3 weeks) is a very common practice because the studied region is a large producer of agricultural products. The averaged 24-h $PM_{2.5}$ value during the biomass burning episodes (from Sep. 28 to Oct. 18) is $239 \pm 163 \mu\text{g}/\text{m}^3$, three times larger than the China's National Air Quality Standard ($75 \mu\text{g}/\text{m}^3$), implying a high health risk from biomass burning aerosols. During the non-biomass-burning seasons, $PM_{2.5}$ remains very low (mean: $31.7 \pm 17.3 \mu\text{g}/\text{m}^3$) although the values are substantially increased during the winter ($47.4 \pm 15.8 \mu\text{g}/\text{m}^3$) due to enhanced fossil-fuel and bio-fuel combustion emissions associated with the extremely cold weather in this region.

3.2. Evidence of fresh biomass-burning aerosol

Water-soluble potassium (K^+) is a widely used marker of biomass burning aerosols (Andreae and Merlet, 2001; Reid et al., 2005). As shown in Fig. 2, episodic events with extremely high $PM_{2.5}$ levels coincides with increases in biomass burning tracer concentrations, such as water-soluble non-sea-salt potassium ($nss-K^+ = K^+ - 0.0355 \times Na^+$) (Lai et al., 2007) from the end of September to the early October. As shown in Fig. 4, a significant linear correlation is found between $PM_{2.5}$ and $nss-K^+$ during the high polluted period, indicating an important biomass burning emission. The emission ratio of $nss-K^+/PM_{2.5}$ from the correlation is 0.026, which is very similar to the average emission ratio (0.024) of $nss-K^+/PM_{2.5}$ derived from open

paddy-residue burning emission residue burning found in the Indo-Gangetic Plain (Rajput et al., 2014). Furthermore, $nss-K^+$ is also significantly correlated ($p < 0.01$, figure not shown) with water-soluble chlorine (Cl^-), suggesting both species are produced from biomass burning emissions.

As shown in Fig. 5, relative abundance of K^+ and Cl^- is increased by a factor of 9 and 13, respectively, during the biomass-burning episodes compared to the non-biomass-burning periods regardless of seasons. Compared to K^+ and Cl^- , the increment of NH_4^+ and NO_3^- are much smaller, whereas SO_4^{2-} levels are even decreased by 30% (Fig. 5). These results clearly indicate that K^+ in biomass burning aerosols is most enriched in KCl particle followed by KNO_3 and/or NH_4NO_3 , and K_2SO_4 are only minor contributors. The high abundance of KCl in biomass burning smoke can be associated with combustion process of the potassium and chloride particles present in the fluids of the vegetation followed by nucleation and condensation of the KCl salt particles (Gaudichet et al., 1995; Lieke et al., 2011). The enhancement of NO_3^- is due to the oxidation of increased NO_x emissions from biomass burning and subsequent reaction with ammonia, leading to formation of ammonium nitrate (NH_4NO_3) particle. Li et al. (2003) suggest that the extent of aging of biomass-burning aerosols can be inferred from relative abundance of the different potassium salts components such as KCl, K_2SO_4 and KNO_3 (Li et al., 2003). A fresh biomass-burning plume is often characterized by high potassium chloride contents, whereas aged biomass-burning smoke is often characterized by potassium sulfate and/or nitrate (Li et al., 2003). The distribution of major inorganic ions observed in this study suggests that the biomass burning aerosols are generally fresh and less aged in Sanjiang Plain, Northeast China (Fig. 5).

3.3. Temporal variation of carbonaceous components and the emission ratios

Fig. 6 displays the temporal variation of carbonaceous components during the sampling period. Concentrations of carbonaceous particles such as WSOC (WSOC), water-insoluble OC (i.e., WIOC = OC-WSOC)

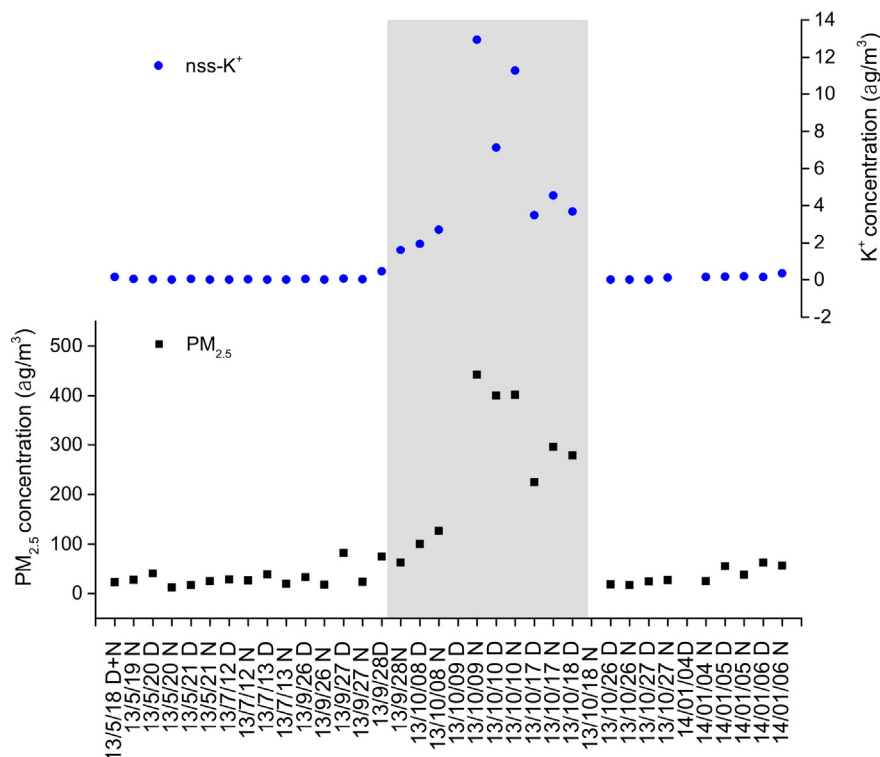
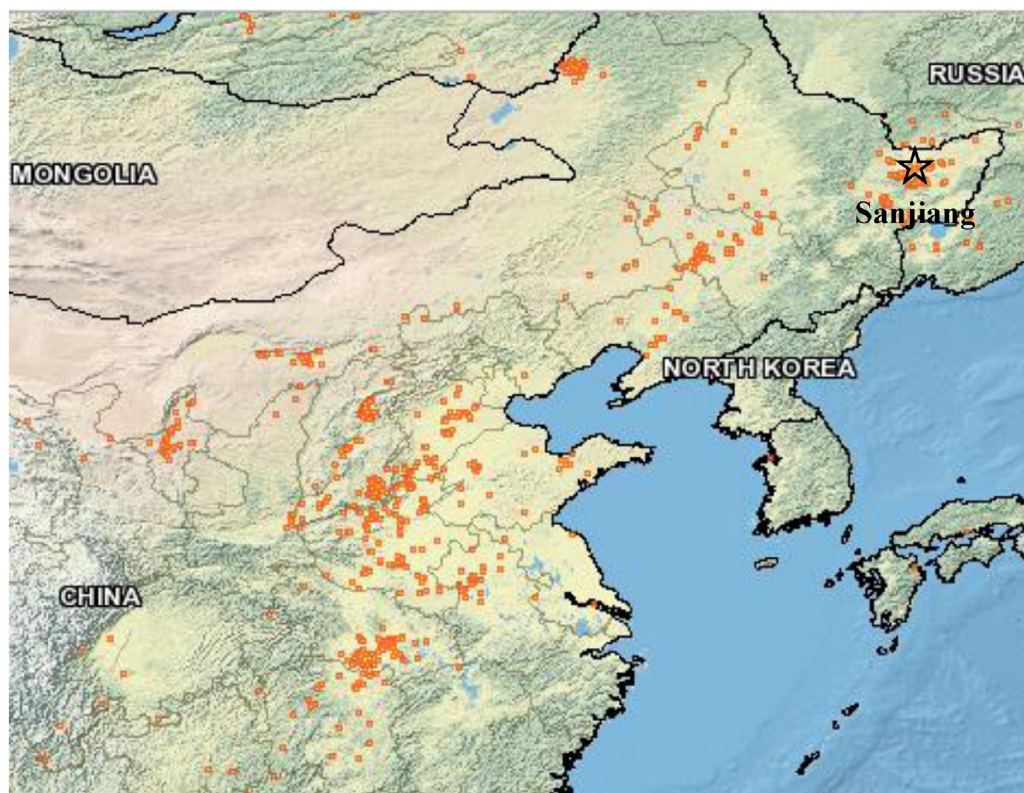
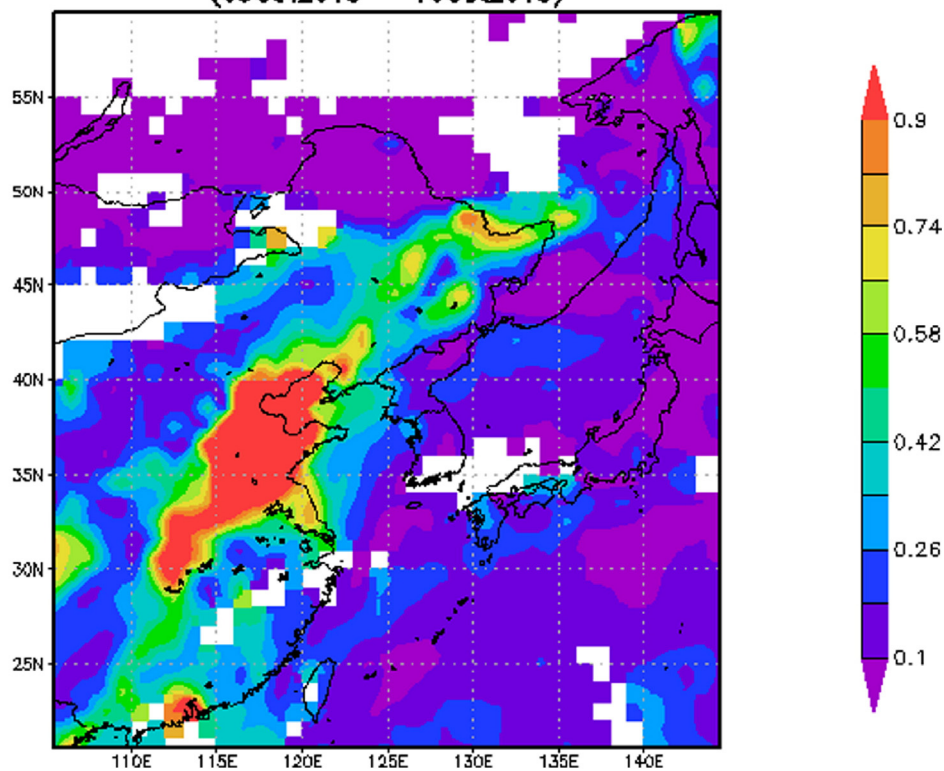


Fig. 2. Temporal variations of non-sea-salt potassium ($nss-K^+$) (top) and $PM_{2.5}$ mass concentrations (bottom) during the sampling period in Sanjiang Plain, Northeast China. Shaded area represents the biomass burning periods. D and N denote daytime and nighttime, respectively.



(a)

MYD08_D3.051 Aerosol Optical Depth at 550 nm [unitless]
(09Oct2013 – 10Oct2013)



(b)

Fig. 3. MODIS fire counts on October 9–10, 2013 (a) and MODIS Terra aerosol optical depth (AOD) at 550 nm on October 9–10, 2013 (b). Active fire locations and brightness were obtained from the Fire Information for Resource Management System (FIRMS) derived from the Moderate Resolution Imaging Spectroradiometer (MODIS).

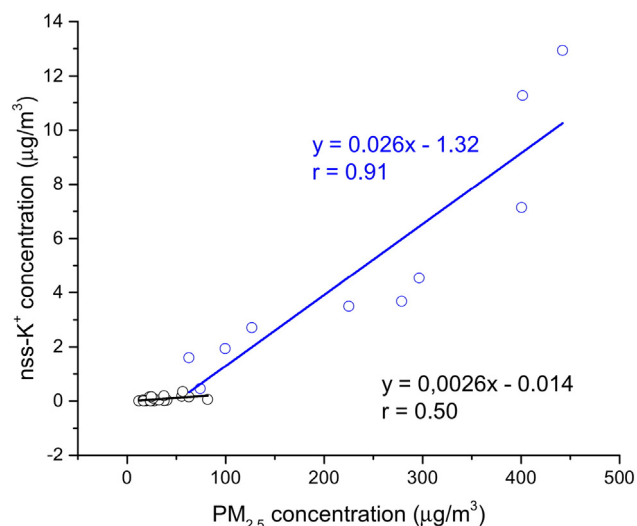


Fig. 4. Linear relationship of non-sea-salt potassium (nss-K^+) and $\text{PM}_{2.5}$ mass concentrations ($\mu\text{g}/\text{m}^3$). The blue line denotes a linear regression fit of the aerosol samples collected during biomass burning episodes whereas the black line denotes a linear regression fit of the aerosol samples collected during non-biomass-burning days. (For interpretation of the references to color in this figure legend, the reader is referred to the web version of this article.)

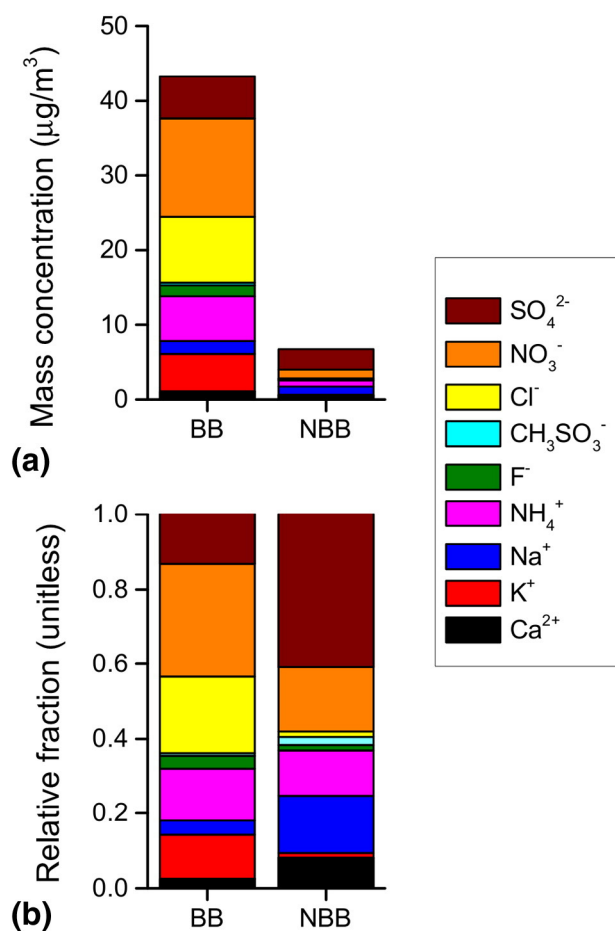


Fig. 5. Average mass concentrations ($\mu\text{g}/\text{m}^3$) (a) and relative abundances (b) of major water-soluble ions in ambient $\text{PM}_{2.5}$ samples collected in Sanjiang Plain, Northeast China during the biomass burning (BB) and non-biomass-burning (NBB) periods.

and EC are 4–12 times higher in the biomass-burning periods than in the non-biomass burning periods. A strong positive correlations is observed between nss-K^+ and carbonaceous components such as OC, EC and WSOC ($p < 0.01$, figures not shown) during the biomass burning episodes, suggesting an important contribution of crop residues burning to carbonaceous aerosols during this biomass burning period. From the linear regression analysis, the ratios of OC/EC, $\text{nss-K}^+/\text{OC}$, $\text{nss-K}^+/\text{EC}$ and WSOC/OC for the agricultural-residue burning emissions are estimated as 10.4 ± 0.5 , 0.054 ± 0.006 , 0.57 ± 0.07 and 0.48 ± 0.01 , respectively. The OC/EC ratio of 10.4 obtained in this study is significantly higher than that for the wheat-residue burning (3.0), but is similar to the previously reported ratio in paddy-residue burning (10.6) (Rajput et al., 2014). The $\text{nss-K}^+/\text{OC}$ ratio of 0.054 suggest high abundance of OC in biomass burning aerosols.

Moreover, OC is almost equally shared by WSOC and WIOC in biomass-burning aerosols. A substantially higher WSOC/OC ratio (on average about 0.66) has been found during the biomass-burning season in the Brazilian Amazon region (Mayol-Bracero et al., 2002). Higher water-soluble fraction of OC could be due to primary production as well as secondary OC formation and/or organic aerosols aging in the tropical climate (Mayol-Bracero et al., 2002). The lower WSOC/OC ratios further support our previous findings (see Section 3.2) that the aerosol samples collected during the biomass-burning season in Sanjiang are most likely derived from fresh or less-aged biomass burning emissions. Furthermore, a similar WSOC/OC ratio (i.e., 0.52 ± 0.02) from a paddy-residue burning is also observed in the Indo-Gangetic Plain (Rajput et al., 2014). There is no significant difference (t-test, $p > 0.05$) found for the emissions ratios (WSOC/OC, OC/EC, $\text{nss-K}^+/\text{OC}$, $\text{nss-K}^+/\text{EC}$) between daytime and nighttime samples, although atmospheric conditions in daytime with relatively high temperature and O_3 concentrations are thought to be more favorable for SOA formation. This similarity again indicates that secondary production of OC is not significant and the aerosols are fresh and less aged. Instead, regional influence and primary production of carbonaceous components may be more pronounced.

3.4. Stable carbon isotopic composition of total carbon

$\delta^{13}\text{C}$ values of aerosol TC range from -27.6‰ to -19.5‰ with a mean of -24.2‰ (Fig. 6). A lower $\delta^{13}\text{C}$ values (mean: -26.2‰) is observed from late September to early October when the elevated $\text{PM}_{2.5}$ and TC values are also observed (Fig. 5). A similar $\delta^{13}\text{C}$ value ($-25.8 \pm 0.5\text{‰}$) has also been reported for aerosols collected in the C3 plant dominated region (Martinelli et al., 2002). It should be noted that aerosols from C4 plant combustion over Amazonia is characterized by larger $\delta^{13}\text{C}$ values ($\delta^{13}\text{C} = -11.5\text{‰}$ to -13.5‰) due to different photosynthetic pathways (Martinelli et al., 2002). The fraction of C3 and C4 plants combustion to TC in the biomass burning seasons is further calculated by:

$$\delta^{13}\text{C}(\text{BB aerosols}) = f(\text{C3}) * \delta^{13}\text{C}(\text{C3}) + f(\text{C4}) * \delta^{13}\text{C}(\text{C4}) + f(\text{others}) * \delta^{13}\text{C}(\text{NBB aerosols})$$

$$f(\text{C3}) + f(\text{C4}) + f(\text{others}) = 1$$

$$f(\text{others}) = \text{TC}(\text{NBB})/\text{TC}(\text{BB})$$

where $\delta^{13}\text{C}(\text{BB aerosols})$ and $\delta^{13}\text{C}(\text{NBB aerosols})$ is the measured $\delta^{13}\text{C}$ in TC of aerosol samples in the biomass burning (BB) episodes and non-biomass-burning (NBB) periods, respectively. $f(\text{C3})$, $f(\text{C4})$ and $f(\text{others})$ refer to the mean fraction of TC from the burning of C3, C4 plants and other emission sources, respectively. $f(\text{others})$ is estimated as the ratio of TC during the non-biomass-burning seasons and the biomass burning episodes assuming that the TC increment during the biomass burning episodes is almost exclusively from biomass burning. $\delta^{13}\text{C}(\text{C3})$ and $\delta^{13}\text{C}(\text{C4})$ are the stable carbon isotope ratios of C₃ and C₄

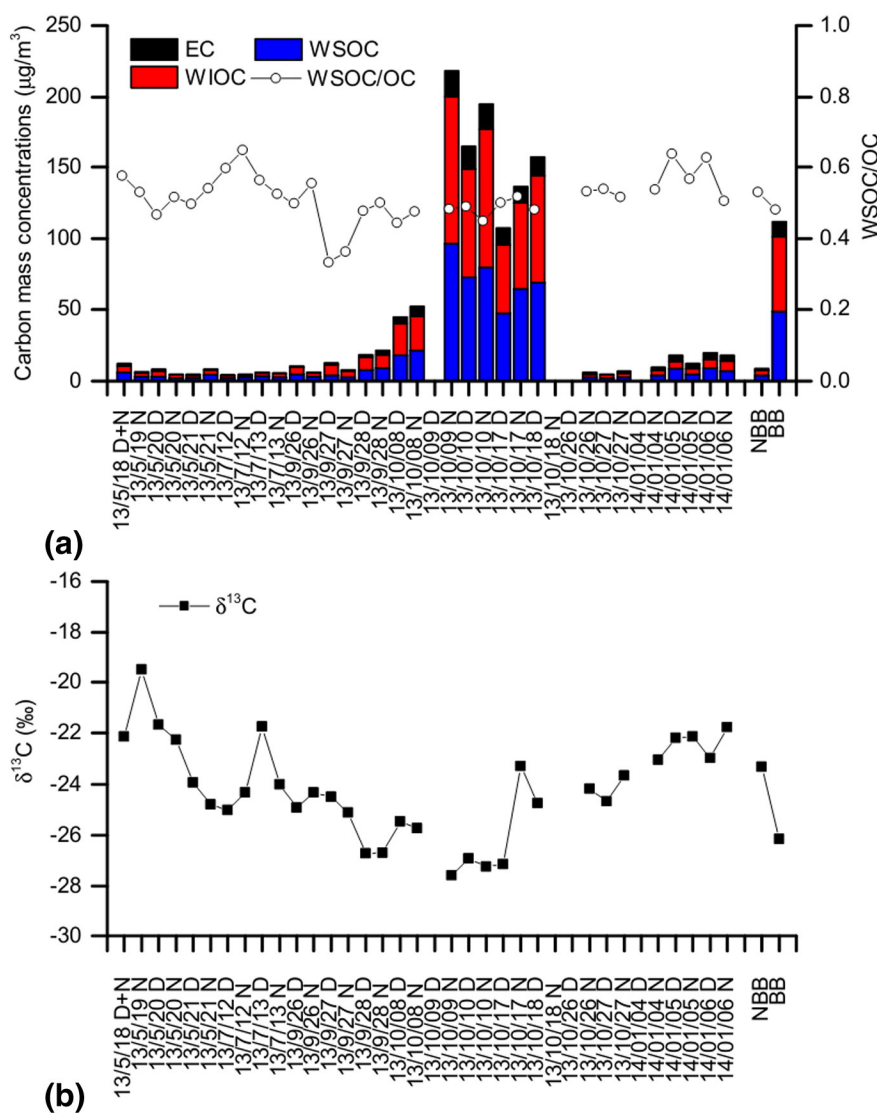


Fig. 6. Temporal variations of mass concentrations of carbonaceous components including water-soluble organic carbon (WSOC), water-insoluble organic carbon (i.e., WIOC = OC-WSOC) and elemental carbon (EC) as well as the WSOC-to-OC ratio (WSOC/OC) (a) and stable carbon isotope composition ($\delta^{13}\text{C}$) of aerosol TC (b). D and N denote daytime and nighttime, respectively. Averaged results during the biomass burning (BB) and non-biomass-burning (NBB) periods are also shown.

plants, respectively, of which the end members are $-30.5 \pm 1.5\%$ and $-12.5 \pm 1\%$ (Martinelli et al., 2002).

Using above equations, average contributions of burning C3 and C4 plants to TC during the biomass burnings seasons are therefore estimated as $83 \pm 18\%$ and $7 \pm 3\%$, respectively. The dominant contribution from C3 plant combustion could be due to the larger land areas planted with rice and wheat compared to C4 plant (i.e. corn) during the autumn in the studied region. During the harvest season in autumn, agricultural waste from the main crops such as rice, wheat and maize in the Sanjiang plain are usually burned openly, contributing significantly to aerosols loading. The results of the stable carbon isotope compositions and emission ratios (see Sections 3.2 and 3.3) further demonstrate that biomass burning aerosol in Sanjiang is dominated by the combustion of rice residues with minor contributions from the burning of wheat and corn residues. $\delta^{13}\text{C}$ values of aerosol TC have recently been reported to increase with the extent of organic aerosols aging (Aggarwal et al., 2013). However, for the Sanjiang aerosols, no significant correlation is found between WSOC/OC (a proxy of organic aerosols aging) between $\delta^{13}\text{C}$ of TC for the biomass burning aerosols, indicating that organic aerosols during the biomass burning seasons is mostly from primary emission in accordance with our previous discussions.

4. Conclusions

PM_{2.5} samples were collected during May 2013 to Jan. 2014 at a background rural site in Sanjiang Plain, Northeast China. Intensively open biomass burning episodes were identified by satellite maps such as MODIS fire and AOD maps. Water-soluble inorganic ions, carbonaceous components and stable carbon isotope compositions were characterized for the biomass burning aerosols. During the biomass burning episode, concentration of PM_{2.5} and carbonaceous components (i.e., OC, EC and WSOC) are significantly enhanced compared to those during non-biomass-burning periods. The enrichment of the non-sea-salt potassium and chlorine is significantly larger than the other inorganic components such as NO_3^- , NH_4^+ , SO_4^{2-} , suggesting the biomass burning aerosols in Sanjiang Plain is mostly fresh or less aged. This is further supported by a relatively lower WSOC/OC ratio compared to that reported in biomass burning aerosols in tropical regions. The emission ratios of OC/EC, $\text{nss-K}^+/\text{OC}$, $\text{nss-K}^+/\text{EC}$ and WSOC/OC for the agricultural-residue burning determined in our study are comparable to those reported for aerosols emitted from paddy-waste combustion in India. $\delta^{13}\text{C}$ values of aerosol TC range from -27.6% to -19.5% with a lower average value ($-26.2\% \pm 1.3\%$) when the elevated

PM_{2.5} and TC values are observed, supporting that the most important source is biomass burning emissions. By conjunction of the emission ratios and stable carbon isotope ratios, biomass-burning aerosols in Sanjiang are mainly from the combustion of rice residues, and the wheat and corn residues are only minor contributors.

Acknowledgments

This work was funded by the Natural Science Foundation for Young Scientists of Jiangsu Province, China (BK20150895), and the Startup Foundation for Introducing Talent of NUIST (Nos. 2015r023 and 2015r019).

References

- Aggarwal, S.G., Kawamura, K., Umarji, G.S., Tachibana, E., Patil, R.S., Gupta, P.K., 2013. Organic and inorganic markers and stable C-, N-isotopic compositions of tropical coastal aerosols from megacity Mumbai: sources of organic aerosols and atmospheric processing. *Atmos. Chem. Phys.* 13, 4667–4680.
- Andreae, M.O., Merlet, P., 2001. Emission of trace gases and aerosols from biomass burning. *Glob. Biogeochem. Cycles* 15, 955–966.
- Birch, M.E., Cary, R.A., 1996. Elemental carbon-based method for monitoring occupational exposures to particulate diesel exhaust. *Aerosol Sci. Technol.* 25, 221–241.
- Cao, G., Zhang, X., Wang, Y., Zheng, F., 2008. Estimation of emissions from field burning of crop straw in China. *Chin. Sci. Bull.* 53, 784–790.
- Cao, J.J., Zhu, C.S., Tie, X.X., Geng, F.H., Xu, H.M., Ho, S.S.H., Wang, G.H., Han, Y.M., Ho, K.F., 2013. Characteristics and sources of carbonaceous aerosols from Shanghai, China. *Atmos. Chem. Phys.* 13, 803–817.
- Cheng, Y., Engling, G., He, K.B., Duan, F.K., Ma, Y.L., Du, Z.Y., Liu, J.M., Zheng, M., Weber, R.J., 2013. Biomass burning contribution to Beijing aerosol. *Atmos. Chem. Phys.* 13, 7765–7781.
- Cheng, Z., Wang, S., Fu, X., Watson, J.G., Jiang, J., Fu, Q., Chen, C., Xu, B., Yu, J., Chow, J.C., Hao, J., 2014. Impact of biomass burning on haze pollution in the Yangtze River delta, China: a case study in summer 2011. *Atmos. Chem. Phys.* 14, 4573–4585.
- Dai, S., Bi, X., Chan, L.Y., He, J., Wang, B., Wang, X., Peng, P., Sheng, G., Fu, J., 2015. Chemical and stable carbon isotopic composition of PM_{2.5} from on-road vehicle emissions in the PRD region and implications for vehicle emission control policy. *Atmos. Chem. Phys.* 15, 3097–3108.
- Fisseha, R., Saurer, M., Jäggi, M., Siegwolf, R.T.W., Dommen, J., Szidat, S., Samburova, V., Baltensperger, U., 2009. Determination of primary and secondary sources of organic acids and carbonaceous aerosols using stable carbon isotopes. *Atmos. Environ.* 43, 431–437.
- Fu, P., Kawamura, K., Chen, J., Li, J., Sun, Y., Liu, Y., Tachibana, E., Aggarwal, S., Okuzawa, K., Tanimoto, H., 2012. Diurnal variations of organic molecular tracers and stable carbon isotopic composition in atmospheric aerosols over Mt. Tai in the North China Plain: an influence of biomass burning. *Atmos. Chem. Phys.* 12, 8359–8375.
- Gaudichet, A., Echalar, F., Chatenet, B., Quisefit, J.P., Malingre, G., Cachier, H., Buatmenard, P., Artaxo, P., Maenhaut, W., 1995. Trace-elements in tropical African savanna biomass burning aerosols. *J. Atmos. Chem.* 22, 19–39.
- Huang, K., Fu, J.S., Hsu, N.C., Gao, Y., Dong, X., Tsay, S.-C., Lam, Y.F., 2013. Impact assessment of biomass burning on air quality in southeast and east Asia during BASE-ASIA. *Atmos. Environ.* 78, 291–302.
- IPCC: Climate Change 2013: The Physical Science Basis. Contribution of Working Group I to the Fifth Assessment Report of the Intergovernmental Panel on Climate Change, Cambridge University Press, Cambridge, United Kingdom and New York, NY, USA, 1535 pp., 2013.
- Jimenez, J.L., Canagaratna, M.R., Donahue, N.M., Prevot, A.S.H., Zhang, Q., Kroll, J.H., DeCarlo, P.F., Allan, J.D., Coe, H., Ng, N.L., Aiken, A.C., Docherty, K.S., Ulbrich, I.M., Grieshop, A.P., Robinson, A.L., Duplissy, J., Smith, J.D., Wilson, K.R., Lanz, V.A., Hueglin, C., Sun, Y.L., Tian, J., Laaksonen, A., Raatikainen, T., Rautiainen, J., Vaattovaara, P., Ehn, M., Kulmala, M., Tomlinson, J.M., Collins, D.R., Cubison, M.J., Dunlea, E.J., Huffman, J.A., Onasch, T.B., Alfarra, M.R., Williams, P.I., Bower, K., Kondo, Y., Schneider, J., Drewnick, F., Borrmann, S., Weimer, S., Demerjian, K., Salcedo, D., Cottrell, L., Griffin, R., Takami, A., Miyoshi, T., Hatakeyama, S., Shimojo, A., Sun, J.Y., Zhang, Y.M., Dzepina, K., Kimmel, J.R., Sueper, D., Jayne, J.T., Herndon, S.C., Trimborn, A.M., Williams, L.R., Wood, E.C., Middlebrook, A.M., Kolb, C.E., Baltensperger, U., Worsnop, D.R., 2009. Evolution of organic aerosols in the atmosphere. *Science* 326, 1525–1529.
- Jung, J., Kawamura, K., 2011. Springtime carbon emission episodes at the Gosan background site revealed by total carbon, stable carbon isotopic composition, and thermal characteristics of carbonaceous particles. *Atmos. Chem. Phys.* 11, 10911–10928.
- Kawamura, K., Tachibana, E., Okuzawa, K., Aggarwal, S.G., Kanaya, Y., Wang, Z.F., 2013. High abundances of water-soluble dicarboxylic acids, ketocarboxylic acids and alpha-dicarbonyls in the mountaintop aerosols over the North China Plain during wheat burning season. *Atmos. Chem. Phys.* 13, 8285–8302.
- Kundu, S., Kawamura, K., Andreae, T.W., Hoffer, A., Andreae, M.O., 2010. Molecular distributions of dicarboxylic acids, ketocarboxylic acids and alpha-dicarbonyls in biomass burning aerosols: implications for photochemical production and degradation in smoke layers. *Atmos. Chem. Phys.* 10, 2209–2225.
- Lai, S.C., Zou, S.C., Cao, J.J., Lee, S.C., Ho, K.F., 2007. Characterizing ionic species in PM_{2.5} and PM₁₀ in four Pearl River Delta cities, South China. *J. Environ. Sci.* 19, 939–947.
- Li, J., Pósfai, M., Hobbs, P.V., Buseck, P.R., 2003. Individual aerosol particles from biomass burning in southern Africa: 2, compositions and aging of inorganic particles. *J. Geophys. Res.* 108, 8484.
- Lieke, K., Kandler, K., Scheuven, D., Emmel, C., Von Glahn, C., Petzold, A., Weinzierl, B., Veira, A., Ebert, M., Weinbruch, S., Schutz, L., 2011. Particle chemical properties in the vertical column based on aircraft observations in the vicinity of Cape Verde Islands. *Tellus B Chem. Phys. Meteorol.* 63, 497–511.
- Martinelli, L.A., Camargo, P.B., Lara, L.B.L.S., Victoria, R.L., Artaxo, P., 2002. Stable carbon and nitrogen isotopic composition of bulk aerosol particles in a C4 plant landscape of southeast Brazil. *Atmos. Environ.* 36, 2427–2432.
- Mayol-Bracero, O.L., Guyon, P., Graham, B., Roberts, G., Andreae, M.O., Decesari, S., Facchini, M.C., Fuzzi, S., Artaxo, P., 2002. Water-soluble organic compounds in biomass burning aerosols over Amazonia – 2. Apportionment of the chemical composition and importance of the polyacidic fraction. *J. Geophys. Res.* 107, D8091.
- Mkoma, S.L., Kawamura, K., Tachibana, E., Fu, P.Q., 2014. Stable carbon and nitrogen isotopic compositions of tropical atmospheric aerosols: sources and contribution from burning of C-3 and C-4 plants to organic aerosols. *Tellus B Chem. Phys. Meteorol.* 66.
- Pope III, C.A., Dockery, D.W., 2006. Health effects of fine particulate air pollution: lines that connect. *J. Air Waste Manage. Assoc.* 56, 709–742.
- Pöschl, U., 2005. Atmospheric aerosols: composition, transformation, climate and health effects. *Angew. Chem., Int. Ed.* 44, 7520–7540.
- Qin, X.L., Yan, H., Zhan, Z.H., Li, Z.Y., 2014. Characterising vegetative biomass burning in China using MODIS data. *Int. J. Wildland Fire* 23, 69–77.
- Rajput, P., Sarin, M., Sharma, D., Singh, D., 2014. Characteristics and emission budget of carbonaceous species from post-harvest agricultural-waste burning in source region of the Indo-Gangetic Plain. *Tellus B Chem. Phys. Meteorol.* 66.
- Reid, J.S., Koppmann, R., Eck, T.F., Eleuterio, D.P., 2005. A review of biomass burning emissions part II: intensive physical properties of biomass burning particles. *Atmos. Chem. Phys.* 5, 799–825.
- Sang, X.F., Zhang, Z.S., Chan, C.Y., Engling, G., 2013. Source categories and contribution of biomass smoke to organic aerosol over the southeastern Tibetan Plateau. *Atmos. Environ.* 78, 113–123.
- Tiunov, A.V., 2007. Stable isotopes of carbon and nitrogen in soil ecological studies. *Biol. Bull.* 34, 395–407.
- Wang, Z., Song, K., Ma, W., Ren, C., Zhang, B., Liu, D., Chen, J., Song, C., 2011. Loss and fragmentation of marshes in the Sanjiang Plain, Northeast China, 1954–2005. *Wetlands* 31, 945–954.
- Widory, D., Roy, S., Le Moullec, Y., Goupil, G., Cocherie, A., Guerrot, C., 2004. The origin of atmospheric particles in Paris: a view through carbon and lead isotopes. *Atmos. Environ.* 38, 953–961.
- Zhang, G., Li, J., Li, X.D., Xu, Y., Guo, L.L., Tang, J.H., Lee, C.S.L., Liu, X.A., Chen, Y.J., 2010a. Impact of anthropogenic emissions and open biomass burning on regional carbonaceous aerosols in South China. *Environ. Pollut.* 158, 3392–3400.
- Zhang, Y.-L., Li, J., Zhang, G., Zotter, P., Huang, R.-J., Tang, J.-H., Wacker, L., Prévôt, A.S.H., Szidat, S., 2014. Radiocarbon-based source apportionment of carbonaceous aerosols at a regional background site on Hainan Island, South China. *Environ. Sci. Technol.* 48, 2651–2659.
- Zhang, Z.S., Engling, G., Lin, C.Y., Chou, C.C.K., Lung, S.C.C., Chang, S.Y., Fan, S.J., Chan, C.Y., Zhang, Y.H., 2010b. Chemical speciation, transport and contribution of biomass burning smoke to ambient aerosol in Guangzhou, a mega city of China. *Atmos. Environ.* 44, 3187–3195.
- Zhao, H.M., Tong, D.Q., Gao, C.Y., Wang, G.P., 2015. Effect of dramatic land use change on gaseous pollutant emissions from biomass burning in Northeastern China. *Atmos. Res.* 153, 429–436.